Effect of Bed Thickness on the Segregation Behavior of Particle Mixtures in a Gas Fluidized Bed

ARTICLE *in* INDUSTRIAL & ENGINEERING CHEMISTRY RESEARCH · FEBRUARY 2010

Impact Factor: 2.59 · DOI: 10.1021/ie901478a

2 AUTHORS:

Yuqing Feng
University of New South Wales
48 PUBLICATIONS **466** CITATIONS
SEE PROFILE

Aibing Yu
University of New South Wales
621 PUBLICATIONS **11,686** CITATIONS
SEE PROFILE

Effect of Bed Thickness on the Segregation Behavior of Particle Mixtures in a Gas Fluidized Bed

Y. Q. Feng[†] and A. B. Yu*

Laboratory for Computer Simulation and Modelling of Particulate Systems, School of Materials Science and Engineering, The University of New South Wales, Sydney, NSW 2052, Australia

Discrete particle simulation has been recognized as a useful numerical technique to elucidate the fundamentals of particle−fluid flow, in particular, gas fluidization. In general, it is achieved by combining discrete element method (DEM) for solid flow with computational fluid dynamics (CFD) for continuum gas. Limited by computational capability, such studies are mainly conducted using a two-dimensional (2D) bed in which particles are treated as discs or a pseudo-three-dimensional (3D) bed where the bed thickness is the same as the particle diameter. The loss of one-dimensional motion may significantly affect the flow and related behavior. This paper presents a numerical study of the effect of the front and rear walls of a fluidized bed on the mixing and segregation behavior of particle mixtures. Particle diameters used for simulation are 1 mm for flotsam and 2 mm for jetsam, respectively. Numerical simulations are conducted for two beds of different thicknesses, fluidized at different gas velocities. One, referred to as the 2D case, shows the bed thickness is 1.1 times the thickness of the particle diameter of jetsam with the front and rear walls supporting the particles; the other, referred to as the 3D case, shows the bed thickness is 4.05 times the particle diameter of jetsam with the application of periodical boundary conditions to the front and rear walls which simulate the 3D motion of particles in the bed. Comparison conducted in terms of solid flow patterns shows that both 2D and 3D simulations can capture the key features of the mixing/segregation process, but the transient segregation occurs at different velocity ranges. Further comparison is conducted on the basis of microdynamic variables, such as mixing kinetics, interactions between particles and fluid, and between particles, and particle contact numbers. These quantitative comparisons demonstrate a significant difference between 2D and 3D simulations, which indicates the necessity of 3D simulation for engineering application.

1. Introduction

Computational fluid dynamics (CFD) for fluid flow[1] and discrete element method (DEM) for solid flow[2] were developed separately a few decades ago. However, their combined use for modeling a coupled gas−solid flow only appeared in the 1990s.[3] In general, this is achieved by combining DEM for discrete particles with CFD for continuum gas, or the so-called combined continuum and discrete model (CCDM) representing the fact that the nature of such modeling includes a combination of continuum gas and discrete solid flow.[4,5]

In CCDM, the transient behavior of individual particles, such as their trajectories and acting forces, is readily available, making it very useful to study the mechanisms governing different flow behaviors. With the current computational capacity, this method may not be directly used to study most of the industrial processes where millions to billions of particles are present. However, the information obtained from CCDM studies is believed to be useful for fundamental understanding and hence for process design and optimization. Thus, following the earlier developers,[3,4,6] CCDM has increasingly been used to study the fundamentals of various gas−solid flows under different conditions, as reviewed recently.[7,8]

Limited by computational capacity, most of the CCDM studies thus far reported in the literature are conducted using two-dimensional (2D) beds in which particles are treated as discs or pseudo-three-dimensional (3D) beds where the bed thickness is the same as the particle diameter. This treatment can significantly reduce the number of particles and computational time. However, such a 2D study may not represent the 3D phenomena well. For example, there is a significant difference in porosity between a 2D and 3D beds. Hence a high gas velocity has to be used to fluidize a 2D bed. To overcome this problem, the porosity calculated in a 2D bed, ε_{2D}, has been transferred to the corresponding 3D one, ε_{3D}, through some arbitrary treatments; e.g., $\varepsilon_{3D} = 1 - (2/(\pi\sqrt{3})^{1/2})(1 - \varepsilon_{2D})^{3/2}$ [6,9] or $\varepsilon_{3D} = 1 - (\sqrt{2}/(\pi\sqrt{3})^{1/2})(1 - \varepsilon_{2D})^{3/2}$.[10−13] To date, it is not clear to which degree this approach is valid, particularly for systems composed of particles of different sizes as the treatments proposed are for monosized particles only.

On the other hand, it is known that the loss of a one-dimensional motion may affect the flow and related behavior to some extent. This is particularly true for multisized particle systems. However, the quantitative difference between 2D and 3D simulations is not clear. This uncertainty also applies to physical experiments which are often conducted using 2D beds for the convenience of visualization or measurement. There is a risk that such 2D data is directly used in practical application.

This work aims to clarify the application of 2D beds by conducting a detailed numerical study of gas−solid flow in fluidization, focused on a binary particle mixture (1 mm for flotsam and 2 mm for jetsam) in connection with our previous work.[14,15] Numerical simulations are conducted under the same bed geometries except for the bed thickness. One bed is 2D, with its bed thickness being 1.1 times the particle diameter of jetsam, and with the front and rear walls to support particles. The other is 3D, with its bed thickness being 4.05 times the particle diameters of jetsam, and with the application of periodical boundary conditions to the front and rear walls in order to simulate the 3D motion of particles in the bed with a

* To whom correspondence should be addressed. E-mail: A.Yu@unsw.edu.au.

[†] Present address: CSIRO Minerals, P. O. Box 312, Clayton South, Vic 3169, Australia. E-mail: Yuqing.Feng@csiro.au

10.1021/ie901478a
Published on Web 02/25/2010

Table 1. Parameters Used in the 2D and 3D Simulations

solid phase		gas phase and bed geometry	
density (kg m^{-3})	2500	viscosity (kg m^{-1} s^{-1})	1.8×10^{-5}
Young's modulus (N m^{-2})	1.0×10^{8}	density (kg/m^3)	1.205
Poisson ratio (N m^{-2})	0.3	bed	
		width (m)	0.065
sliding friction coefficient	0.3	height (m)	0.26
damping coefficient	0.2	thickness (m)	0.0081 (3D)
jetsam			0.0022 (2D)
diameter (m)	0.002	computational cell	
number	2777 (3D)	width (m)	0.00325
	555 (2D)	height (m)	0.00325
flotsam		time step (s)	2.5×10^{-6}
diameter (m)	0.001		
number	22223 (3D)		
	4445 (2D)		
time step (s)	2.5×10^{-6}		

relatively small number of particles. Comparisons will be made in terms of the solid flow patterns, mixing kinetics, interactions between particles and fluid, and between particles, and contacts between particles.

2. Simulation Method and Conditions

2.1. Simulation Method. The simulation is based on a CCDM model developed at the University of New South Wales, and the details of the approach can be found elsewhere.[14,15] For brevity, therefore, only the key structure of the model is described below.

The solid phase is treated as a discrete phase that is described by a conventional DEM. The translational and rotational motions of a particle at any time, t, in the bed are thus determined by Newton's second law of motion. These can be written as

$$m_i \frac{\mathrm{d}\mathbf{v}_i}{\mathrm{d}t} = \mathbf{f}_{\mathrm{f},i} + \sum_{j=1}^{k_i} (\mathbf{f}_{\mathrm{c},ij} + \mathbf{f}_{\mathrm{d},ij}) + \mathbf{f}_{\mathrm{g},i} \tag{1}$$

$$I_i \frac{\mathrm{d}\boldsymbol{\omega}_i}{\mathrm{d}t} = \sum_{j=1}^{k_i} \mathbf{T}_{ij} \tag{2}$$

where m_i, I_i, k_i, $\mathbf{v}_i$, and $\boldsymbol{\omega}_i$ are respectively the mass, moment of inertia, number of contacting particles, and translational and rotational velocities of particle i; $\mathbf{f}_{\mathrm{f},i}$ and $\mathbf{f}_{\mathrm{g},i}$ are fluid drag force and gravitational force, respectively. $\mathbf{f}_{\mathrm{c},ij}$, $\mathbf{f}_{\mathrm{d},ij}$, and $\mathbf{T}_{i,j}$ are the contact force, viscous contact damping force, and torque between particles i and j. These interparticle forces and torques are summed over the k_i particles in interaction with particle i. The equations to calculate the forces and torques, together with the justification for their usage, can be found from our previous studies.[14−16]

The gas phase is treated as a continuous phase and modeled in a way very similar to the one widely used in the conventional two-fluid model.[17] Thus, the governing equations are the conservation of mass and momentum in terms of the local mean variables over a computational cell, given by

$$\frac{\partial \varepsilon}{\partial t} + \nabla \cdot (\varepsilon \mathbf{u}) = 0 \tag{3}$$

Table 2. Gas Injection Velocities Used in 2D and 3D Simulations

		for given velocity ratio					
		1.217	1.391	1.565	1.739	2.087	2.435
velocity (m/s)	3D	0.7	0.8	0.9	1.0	1.2	1.4
	2D	1.339	1.530	1.722	1.913	2.296	2.678

$$\frac{\partial (\rho_{\mathrm{f}} \varepsilon \mathbf{u})}{\partial t} + \nabla \cdot (\rho_{\mathrm{f}} \varepsilon \mathbf{u}\mathbf{u}) = -\nabla P - \mathbf{F}_{\mathrm{pf}} + \nabla \cdot (\varepsilon \boldsymbol{\tau}) + \rho_{\mathrm{f}} \varepsilon \mathbf{g} \tag{4}$$

where $\mathbf{u}$ and P are respectively the fluid velocity and pressure; $\boldsymbol{\tau}$, ε, and $\mathbf{F}_{\mathrm{pf}} = \sum_{i=1}^{k_c} \mathbf{f}_{\mathrm{f},i}/\Delta V$ are the fluid viscous stress tensor, porosity, and particle−fluid interaction force in a computational cell of volume ΔV and with k_c particles in it.

Note that model B formulation is used in this work, where the so-called fluid drag force is actually the sum of the drag force and pressure gradient force in model A formulation.[15,18] Moreover, the equation to calculate the drag force for individual particles in a particle mixture is not so well established. Here we just used the one extended from monosized particles, i.e., the so-called Di Felice equation.[19] The equation has taken into account the presence of other particles, but it may not be accurate enough for particle mixtures. Recently, there are a few attempts to modify the equation for particle mixtures (see, for example, refs 20−22), but their general application is unclear. Different equations may produce different results. However, since the present work is focused on the comparison between the 2D and 3D treatments, the use of different equations would not affect the final conclusion in this aspect.

Equations 1 and 2 for particle flow can be numerically solved by an explicit time integration method, facilitated by suitable boundary conditions for given flow conditions. Here, the interparticle force models are also applied to the interaction between a particle and a wall, with the corresponding wall properties used. For convenience, a wall is assumed to have

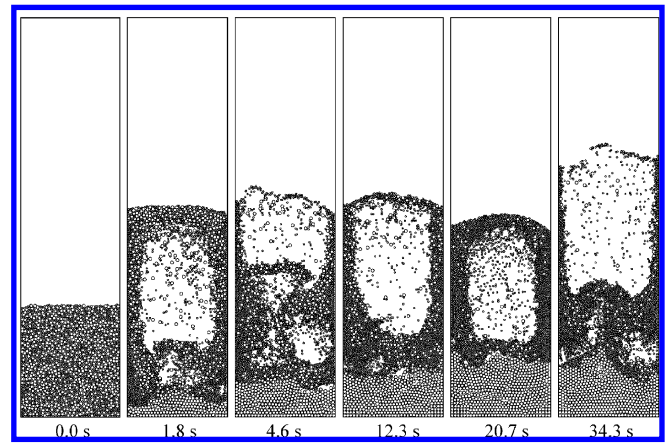

Figure 1. Solid flow patterns of 2D simulation when the gas velocity is 1.913 m/s.

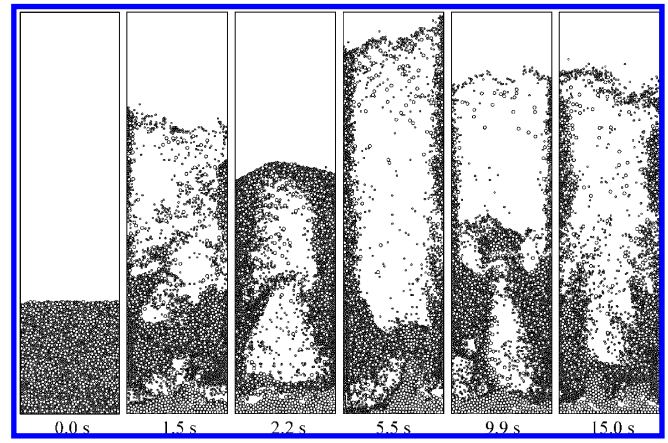

Figure 2. Solid flow patterns from 2D simulation when the gas velocity is 2.678 m/s.

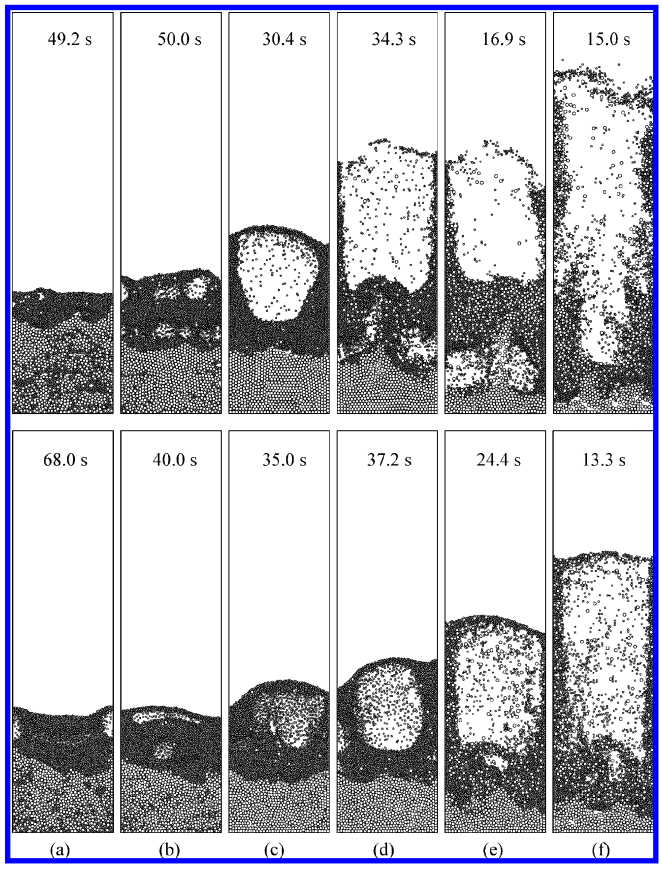

Figure 3. Solid flow patterns of 2D (top) and 3D (bottom) simulations at their respective macroscopically stable states when the gas velocity ratio is (a) 1.217, (b) 1.391, (c) 1.565, (d) 1.739, (e) 2.087, and (f) 2.435.

the same properties as particles. In addition, it is assumed to be so rigid that no displacement and movement results from the particle−wall interaction. On the other hand, eqs 3 and 4 for gas flow can be readily solved by the use of a conventional CFD method. For the present simulation, a no-slip boundary condition is applied to bed walls and a zero normal gradient condition is applied to the top exit for gas velocity while the gas flow at the bottom inlet is specified. These numerical treatments have been widely used in the CCDM studies of gas fluidization published in the literature.

It should be noted that the modeling of the solid flow by DEM is at the individual particle level, while the gas flow by CFD is at the computational cell level. Their coupling is numerically achieved as follows. At each time step, DEM will give information, such as the positions and velocities of individual particles, for the evaluation of porosity and volumetric fluid drag force in a computational cell. CFD will then use this data to determine the gas flow field which then yields the fluid drag forces acting on individual particles. Incorporation of the resulting forces into DEM will produce information about the motion of individual particles for the next time step. The fluid drag force acting on individual particles will react on the fluid phase from the particles, so that Newton's third law of motion is satisfied. The advantage of this coupling technique has been discussed in the previous work.[4,15]

2.2. Simulation Conditions. To examine the wall effect on mixing/segregation behavior, two beds of the same geometry but different thickness are used. The first one has a thickness of 1.1 times the jetsam particle diameter, and the front and back walls are applied to support the particles. Since the motion of jetsam is confined to 2D, this case is referred to as 2D in the following discussion. The other bed, referred to as 3D, has an infinite thickness, achieved by applying the periodical boundary conditions to a bed thickness of 4.05 jetsam particle diameters. This treatment can reduce the number of particles, but still produce 3D results. For comparison, the gas flow in both cases is assumed to be 2D, starting uniformly from the bed bottom. To ensure that the results are comparable, the same bed height is used for the 2D and 3D cases. The flotsam and jetsam are assumed to have the same physical properties, with each counting 50% in volume or weight as they are of the same density. The detailed simulation conditions are listed in Table 1. A simulation is started with the random generation of particles

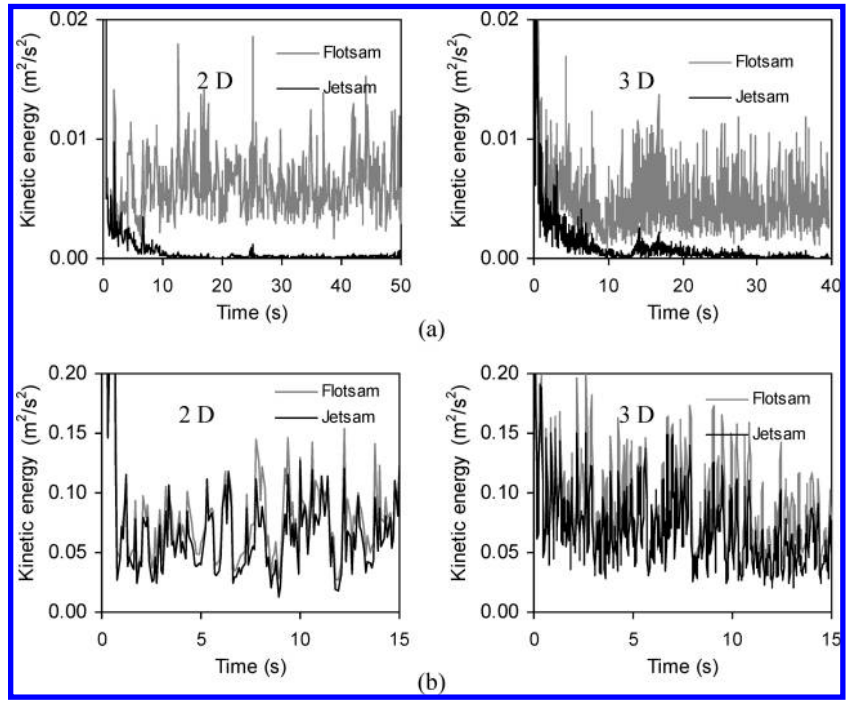

Figure 4. Variation of mean particle kinetic energy when the gas velocity ratio is (a) 1.391 and (b) 2.435.

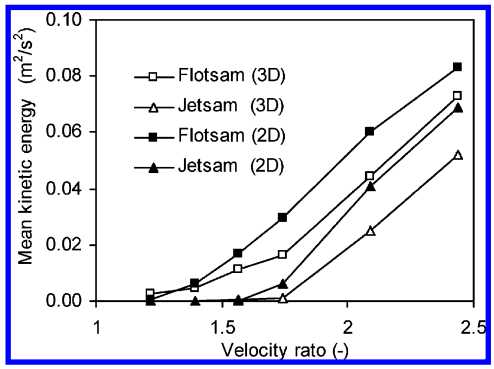

Figure 5. Mean kinetic energy of particles at different velocity ratios when their respective macroscopically stable state is reached.

without particle overlaps in a rectangular bed, followed by a gravitational settling process for 0.6 s. This will produce a packed bed as judged from the negligible velocity of particles. Then, gas is injected at the bottom uniformly to fluidize the bed. Note that the simulation conditions are largely comparable with the studies reported in the literature. So if necessary, some discussion can be made in connection with the previous studies.[14−16]

Obviously, there is a difference in porosity between the 2D and 3D cases. For the binary mixture used in this study, the porosity equals 0.358 and 0.462 respectively corresponding to the well-mixed 3D and 2D packed beds. Thus, comparison between the 2D and 3D cases at a given velocity is unreasonable. For example, at velocity 0.7 m/s, particles are still at the packed state in the 2D simulation while fluidization happens in the 3D simulation. There is a need to identify an acceptable parameter to overcome this difficulty. The arbitrary link between 2D and 3D porosities is not appropriate as discussed above. Here, the ratio of the gas injection velocity to the minimum fluidization velocity, R_g, is selected for this purpose. The minimum fluidization velocity U_{mf} can be calculated on the basis of the mean particle size d (equal to 1.333 mm for both the 2D and 3D cases) and porosity ε. According to the Di Felice equation,[19] $U_{mf} = 0.575$ m/s for the 3D bed and 1.1 m/s for the 2D bed. As segregation appears in a range of gas velocities, 2D and 3D simulations are performed using different velocity ratios as listed in Table 2.

3. Results and Discussion

3.1. Solid Flow Patterns. The mixing/segregation process is strongly affected by gas injection velocities, which can be readily demonstrated by snapshots of solid flow patterns. Figure 1 shows such a segregation process based on the 2D simulation when the gas injection velocity is 1.913 m/s. Following an initial bed expansion, segregation happens gradually. More and more jetsam particles aggregate at the bottom of the bed and stay in a defluidized state. Simultaneously, the flotsam particles aggregate in the top part and remain in a fluidized state where clear bubbles and slugs can be seen. At a microscopic or particle scale, a particle may continuously move up and down, so the bed is always in a dynamic state. However, at a macroscopic scale, the bed as a whole is in a dynamically equilibrium state; this gives the so-called "macroscopically stable state".[14,15] Perfect segregation cannot be achieved when a macroscopically stable state, i.e., the dynamic equilibrium of the gas−solid flow, is reached, due to the existence of the bubbles/slugs which lift the underneath jetsam particles up. When the gas injection velocity is 2.678 m/s, starting with the same initial packing condition, a better mixing state is observed where only insignificant segregation appears at the bottom of the bed (Figure 2).

For the 3D simulations, corresponding to the two velocities as shown in Figures 1 and 2, significant segregation happens at velocity 1.0 m/s and reasonable mixing at 1.4 m/s. The results have been reported in our previous paper;[15] hence, they are not repeated here. Note that the validity of the CCDM used in this work has also been verified in our previous paper.

The final state of mixing/segregation is strongly affected by the gas injection velocity. Figure 3 illustrates the snapshots of solid flow patterns at different velocity ratios when their

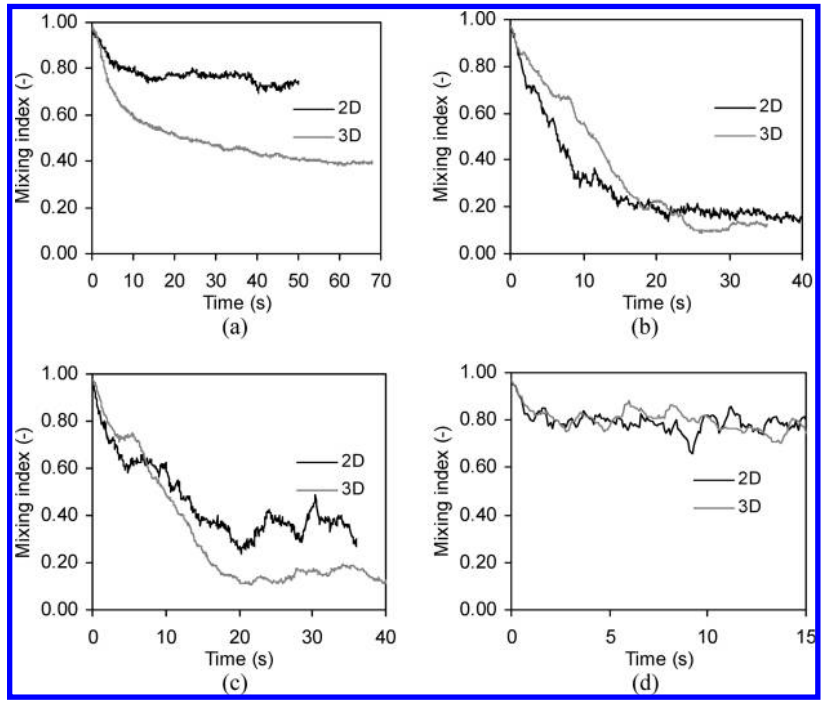

Figure 6. Mixing kinetics when the gas velocity ratio is (a) 1.217, (b) 1.565, (c) 1.739, and (d) 2.435.

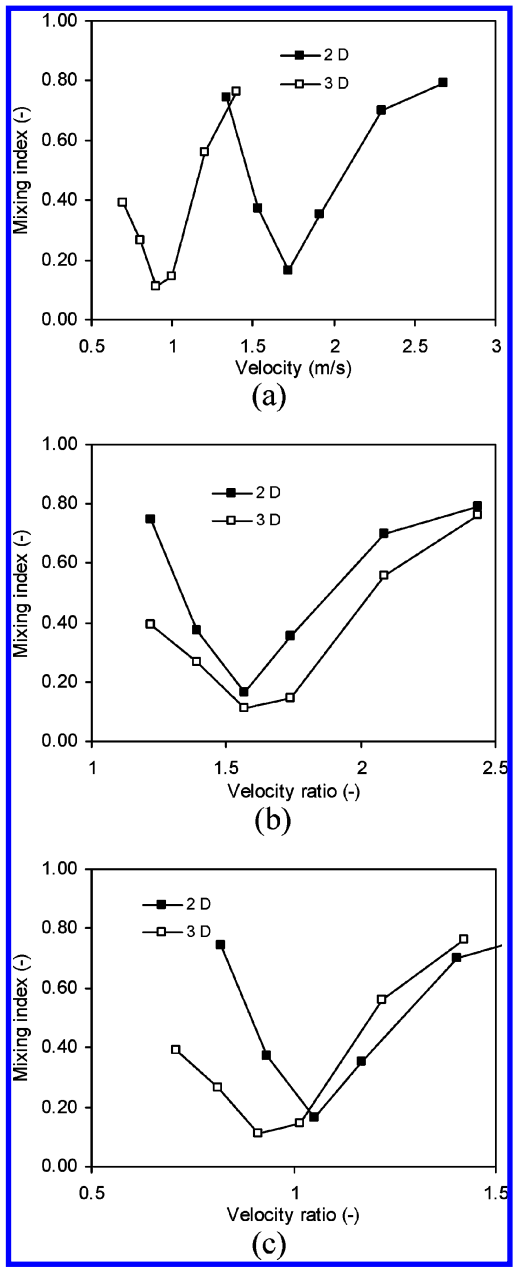

Figure 7. Mean mixing index as a function of (a) gas velocity, (b) gas velocity relative to the minimum fluidization velocity of the particle mixture considered, and (c) gas velocity relative to the minimum fluidization velocity of jetsam particles.

macroscopically stable state is reached. For the 2D simulations, at velocity ratio 1.217, two separate layers can be identified, the concentration of flotsam particles in the bottom layer is significant, and correspondingly the defluidized layer is much higher. The top layer, which is rich in flotsam particles, just reaches its minimum fluidization. At velocity ratio 1.391, the concentration of flotsam particles in the bottom layer becomes smaller and the fluidization of the top layer becomes stronger. This trend becomes more significant at the velocity ratio of 1.565. With further increase of the velocity ratio, the stronger fluidization of the top layer causes more jetsam particles to join in the fluidized layer and at the velocity ratio of 2.435; significant mixing results with only a few jetsam particles aggregating at the bottom. For the 3D simulations, a similar trend is observed. Therefore, it is concluded that the whole picture of the mixing/segregation process can be represented on the basis of both 2D and 3D simulations. However, much larger velocities have to be used to fluidize the bed for 2D simulations. This may cause differences in the microdynamics of the process. Further quantitative comparisons are conducted in this direction, following our previous work,[16] as discussed below.

3.2. Particle Kinetics and Mixing Kinetics. The particle kinetic energy is first calculated for comparison. The spatially averaged value, expressed as $(1/N_{p,i}m_{p,i})\sum_{i=1}^{Np}((1/2)m_{p,i}v_{p,i}^2)$, is calculated for the flotsam and jetsam particles separately, where i is either flotsam or jetsam particle and N_p is the number of one type of particles (flotsam or jetsam). Figure 4 shows the variation of the kinetic energy with time at two velocity ratios. At a velocity ratio of 1.391 m/s (Figure 4a), the mean energy shows a sharp increase due to the bed expansion. Soon afterward, with the rearrangement of particles, the kinetic energy of jetsam decreases due to the segregation, and for flotsam particles, it fluctuates at a higher value. Both the 2D and 3D simulations show such a trend, but give different mean values when their macroscopically stable state is reached. At a high velocity ratio (2.435 here), the mean kinetic energy for flotsam particles and jetsam particles refers to a high value because of the strong fluidization. The value for flotsam particles is a bit higher than that for jetsam particles. This can be clearly seen from the averaged means over a period of time after reaching a macroscopically stable state. The obtained spatial mean kinetic energy is shown in Figure 5. Both 2D and 3D simulations show an increase with the increase of the velocity ratio, and the flotsam gives a higher value than the jetsam. At a given velocity ratio, the 2D simulation shows a much higher value than the 3D simulation for both flotsam and jetsam. This is because a 2D simulation corresponds to a much higher gas injection velocity at the given velocity ratio. The only exception happens at the lower velocity ratios for flotsam particles. At a velocity ratio of 1.217, the 3D simulation shows a higher kinetic energy than the 2D simulation. This is because more flotsam particles join in the top fluidized layer in the 3D simulation than in the 2D simulation at this velocity ratio (Figure 3).

The mixing/segregation process is often quantified in terms of mixing kinetics. Here the so-called Lacey mixing index is used for such quantification. The calculation of Lacey mixing index for a fluidized system has been discussed in our previous paper,[14] which gives a value of 1 for perfect mixing and 0 for a totally segregated state. Figure 6 shows the variation of the mixing index with time at different velocity ratios. At the velocity ratio of 1.217 (Figure 6a), both 2D and 3D simulations show a decrease due to the segregation. However, the difference is significant: the 3D simulation results in a larger degree of segregation and takes a longer time to reach its equilibrium state. When the velocity ratio is 1.565 (Figure 6b), a different rate of segregation is observed but the value is very close at their final state. Figure 6c shows a similar rate of segregation, but a different value at their final state when the velocity ratio is 1.739. At the highest ratio (2.435) used in this simulation, both the 3D and 2D simulations show a high degree of mixing and their value is very close (Figure 6d). This can also be confirmed by checking their flow patterns as shown in Figure 3, where both simulations correspond to a strong fluidization and a better mixing state.

The difference in mixing/segregation kinetics may be related to many factors. In the 2D simulation, the loss of one-dimensional motion will cause less interparticle percolation.[23,24] Therefore, the final degree of mixing will be decreased. While at the same velocity ratio, particles in the 2D simulation are more mobile due to higher gas injection velocity, reflected by

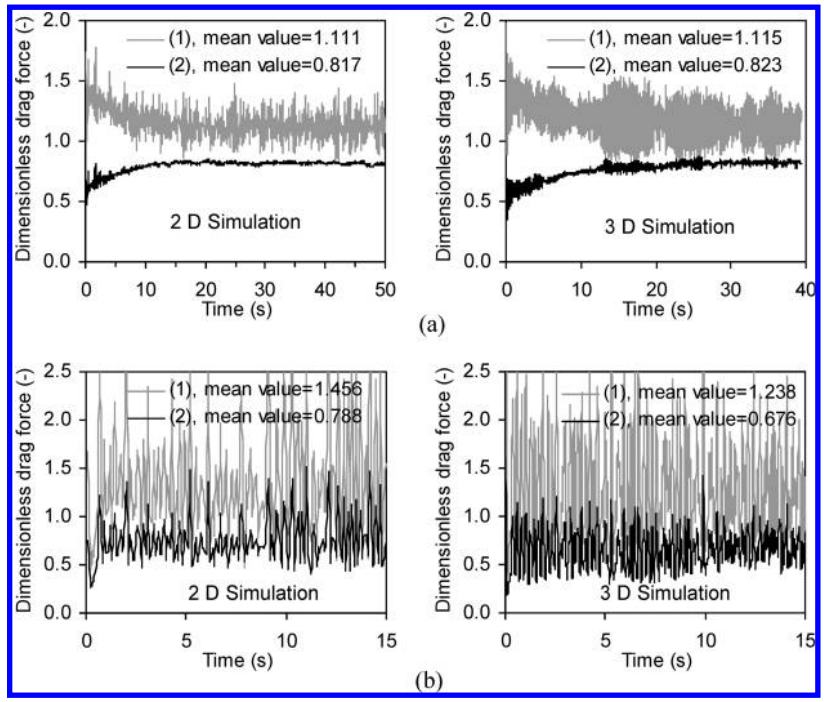

Figure 8. Variation of spatial mean drag force (line 1 for flotsam and line 2 for jetsam) with time when the gas velocity ratio is (a) 1.391 and (b) 2.435.

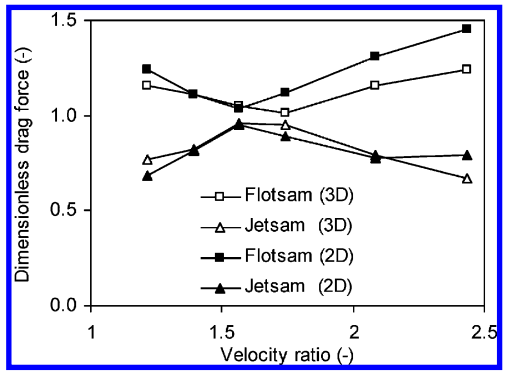

Figure 9. Mean drag force of flotsam and jetsam particles as a function of gas velocity ratio at their respective macroscopically stable state.

the particle kinetic energy shown in Figure 5. A combined effect of these factors contributes to this difference.

At their respective stable state, the time-averaged value of the mixing index is calculated and their variation at different velocities is shown in Figure 7. Both 2D and 3D simulations show a clear "V" curved distribution as a function of velocity ratio, which qualitatively agree with the experimental finding.[25] At a given velocity ratio (Figure 7b), the mixing index from the 3D simulation is a bit lower than that from the 2D simulation, implying more significant segregation from the 3D simulation. If the mixing index is expressed as a function of gas injection velocity, a significant difference can be identified. These appear at different velocity ranges, and the velocity range spans much wider for the 2D simulation than for the 3D simulation (Figure 7a). The results confirm the reasonableness of the velocity ratio for quantitative comparison between 2D and 3D beds. Interestingly, Di Renzo et al.[26] gave a similar suggestion in their study of the mixing/segregation in fluidized beds of two solids differing in particle density.

The minimum fluidization velocity U_{mf} varies with mean particle size d and porosity ε for the given flow conditions. Because of this, different velocity ratios can be defined. For example, for the system considered, the minimum fluidization velocity can be the one corresponding to the large component (or the heavy one as used in ref 26), or the one corresponding to a particle mixture as used in the present study. It would be of interest to know which one is more suitable for the comparison between 2D and 3D treatments. This issue was tested as part of the present study. The data used include the following: $d = 1.333$ mm, $\varepsilon_{2D} = 0.462$ and $U_{mf,2D} = 1.1$ m/s, $\varepsilon_{3D} = 0.358$, and $U_{mf,3D} = 0.575$ m/s for the particle mixture considered; and $d = 2.0$ mm, $\varepsilon_{2D} = 0.481$ and $U_{mf,2D} = 1.635$ m/s, $\varepsilon_{3D} = 0.389$ and $U_{mf,3D} = 0.575$ m/s for the jetsam particles. Examination of the results in Figure 7b,c suggests that the velocity ratio using the minimum fluidization velocity of a particle mixture is a better choice. This explains why it is used in the present analysis.

3.3. Particle−Fluid Interaction and Bed Pressure. Particle−fluid interaction force plays an important role in fluidization, and is therefore examined in detail in this work. The mean value over types of particles in the bed, given as $(1/N_{p,i}m_{p,i}g)\sum_{i=1}^{Np} \mathbf{f}_d$, is calculated separately for flotsam and jetsam and nondimensioned by their respective weight. As the segregation dominantly happens in the vertical direction, only the particle−fluid interaction force in this direction is considered here. Figure 8 shows the evolution of the mean particle fluid drag force acting on flotsam and jetsam particles at two velocity ratios. At velocity ratio 1.391, the mean value is larger than its gravity for flotsam and is lower than its gravity for jetsam. This difference will provide a driving force for the upward motion of flotsam particles and the downward motion of jetsam particles. Following the process of segregation, the mean value decreases for flotsam and increases for jetsam. A macroscopically stable state is reached later, where its mean value just fluctuates around a certain value, which is still larger than its gravity for flotsam but less for jetsam. The above description is applicable for both 2D and 3D simulations; however, the differences observed include the transition time in reaching their dynamically stable state and the time-averaged mean value. When the gas velocity ratio is 2.435 m/s, the fluctuation increases for both 2D and 3D simulations, as well as for both

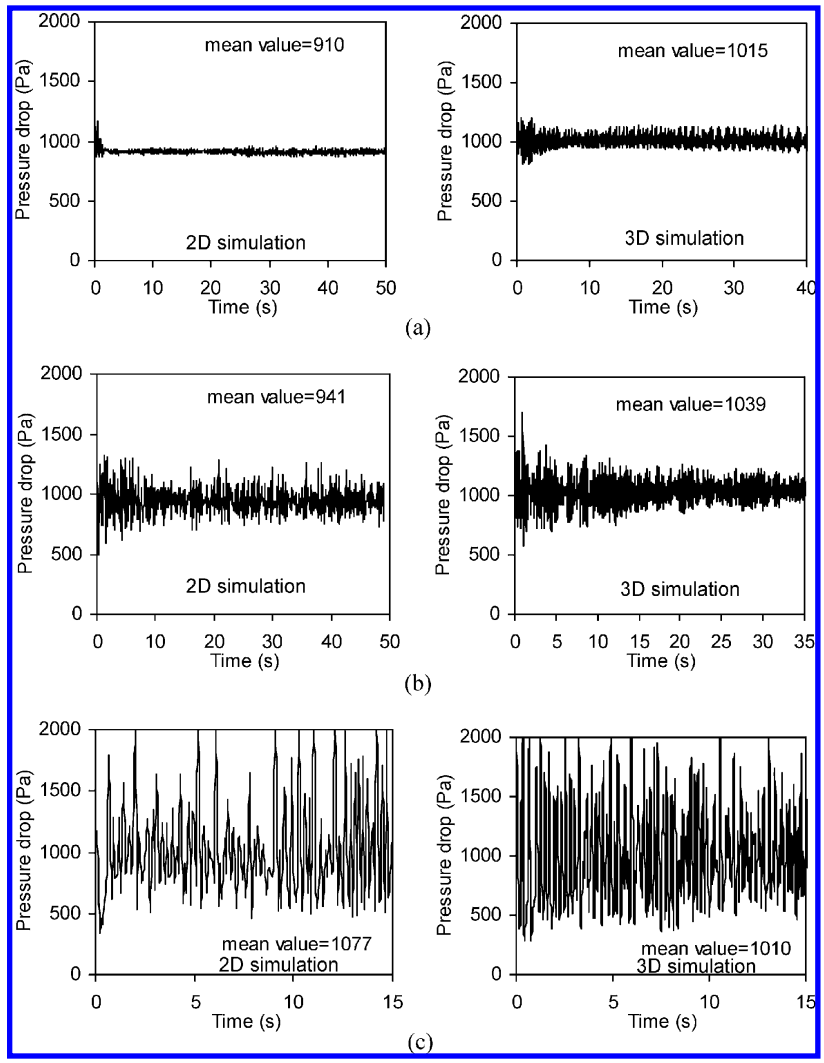

Figure 10. Variation of pressure drop with time when the gas velocity ratio is (a) 1.217, (b) 1.565;, and (c) 2.435.

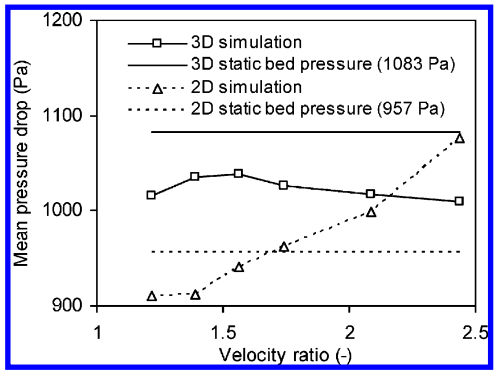

Figure 11. Mean pressure drop at different gas velocity ratios.

flotsam and jetsam. Almost no transition state is observed for both 2D and 3D simulations. Note that the large difference in the fluid drag force between flotsam and jetsam corresponds to a better mixing state. It actually results from the strong interactions between particles.[14]

This variation of fluid drag force can be better demonstrated by plotting their means over a representative period at their respective dynamically stable states. Figure 9 shows the calculated mean values at different velocity ratios. For both 2D and 3D simulations, the time-averaged value for flotsam decreases with the increase of gas velocity. First, it reaches a minimum at velocity ratio of 1.565, which is just slightly higher than its gravity; it then increases with the further increase of gas velocity. On the contrary, for jetsam, the time-averaged value increases first with the increase of gas velocity, where it reaches a maximum at velocity ratio of 1.565, which is just a bit lower than its gravity; then it decreases with the further increase of gas velocity. The differences include the minimum value for flotsam and the maximum value for jetsam, which appear at different velocity ratios. Generally, at low or high ratios, the 2D results are much higher for flotsam and lower for jetsam than the 3D results. However, this is not applicable for jetsam at the higher ratios used in this simulation. At a velocity ratio of 2.296, the mean value for jetsam is identical and the 2D simulation refers to a much higher value than in the 3D simulation.

Figure 10 records the variation of the bed pressure drop with time at different velocity ratios. Obviously, the increase of gas velocities will cause a larger pressure fluctuation for both 2D and 3D simulations. The pressure drop is time-averaged for comparison and is shown in Figure 11. Interestingly, unlike the 3D simulation where the pressure drop is always a bit lower than the bed weight, a continuous increase of pressure drop is observed, and at higher velocity ratios, the pressure drop is even larger than the bed weight for 2D simulations. The reason for a lower pressure drop than its weight can be understood as the bottom wall supports some particles. For 2D simulations, the front and rear walls also interact with particles. These walls

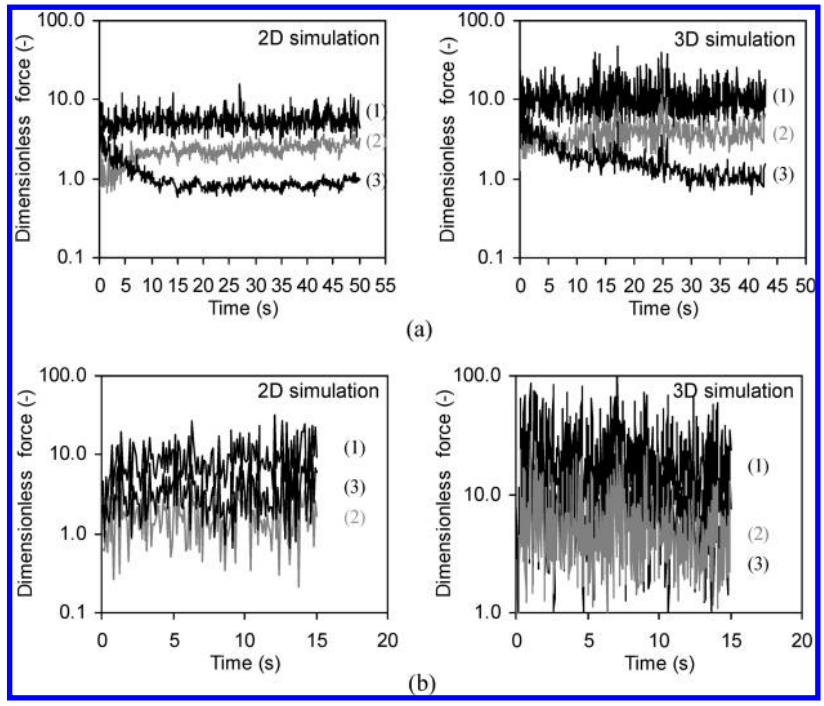

Figure 12. Variation of mean contact force with time (line 1, from flotsam to flotsam; line 2, from jetsam to jetsam; line 3, from flotsam to jetsam) when the gas velocity ratio is (a) 1.391 and (b) 2.435.

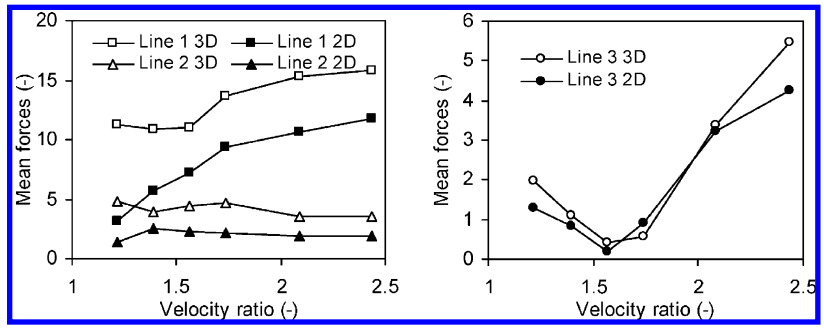

Figure 13. Mean contact force at difference gas velocity ratios: line 1, flotsam to flotsam; line 2, jetsam to jetsam; and line 3, jetsam from flotsam.

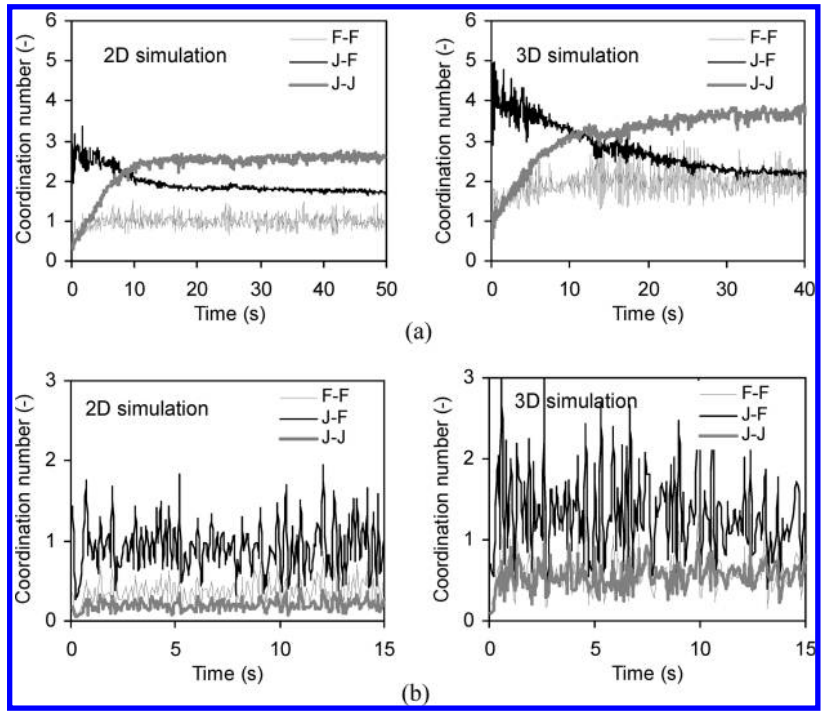

Figure 14. Variation of mean partial coordination number with time when the gas velocity ratio is (a) 1.391 and (b) 2.435.

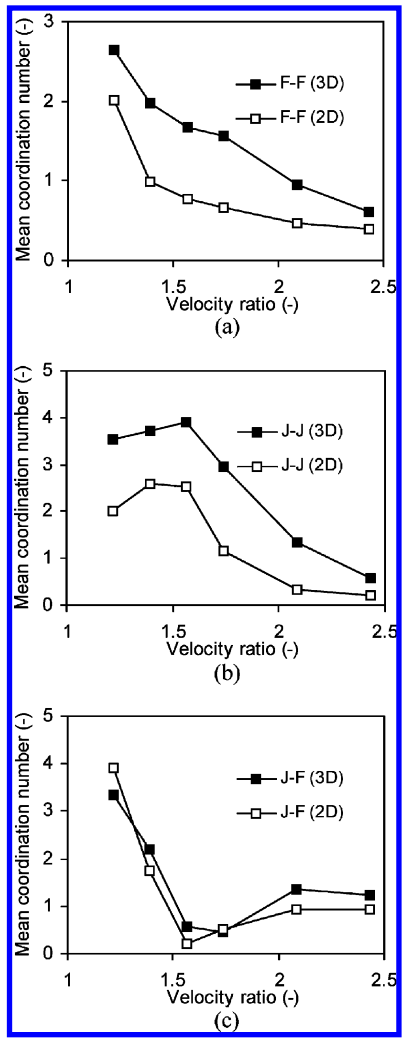

Figure 15. Mean partial coordination numbers at different velocity ratios: (a) flotsam with flotsam, (b) jetsam with jetsam, and (c) jetsam with flotsam.

will cause a suppression of particle motion due to the frictions between particles and wall; hence, a higher pressure drop, corresponding to the mean particle−fluid interaction force, is needed.

3.4. Particle−Particle Interaction and Contact Condition. The wall may also affect the particle−particle interactions. The spatial averaged value, given as $(1/N_p)\sum_{i=1}^{Np}$ $((1/m_{p,i}g)\sum_{j=1}^{k_j}|\mathbf{f}_{cn,ij} + \mathbf{f}_{dn,ij} + \mathbf{f}_{ct,ij} + \mathbf{f}_{dt,ij}|)$, is used for this comparison. k_i is the contact number of one type of particles (either flotsam or jetsam) in contact with particle i. Three kinds of particle contacts (flotsam to flotsam, flotsam to jetsam, and jetsam to jetsam) are calculated individually.

Figure 12 shows the variation of the mean contact force with time for two velocity ratios. At velocity ratio 1.391 (Figure 12a), the contact force of flotsam with other flotsam particles (line 1) fluctuates around a constant value, which is larger than the other two types of contacts. The contact force of jetsam particle with jetsam particles increases (line 2), but the contact force of jetsam with flotsam particles decreases (line 3) as a result of segregation. At velocity ratio 2.435, no transition stage is seen for the three types of contact. The difference between the 2D and 3D simulations can be better highlighted by the time-averaged values as shown in Figure 13. For the contact force between flotsam particles, the 3D simulation produces a higher value than the 2D simulation (line 1). This is also the case for the contact forces between jetsam particles (line 2). The interaction force between jetsam and flotsam particles first decreases, due to the size segregation leading to less contacts, and then increases with the increase of velocity ratios because particle mixing rather than segregation is dominant at a high velocity ratio. The difference between the 2D and 3D simulations is small. The increase of gas injection velocity will increase the intensity of fluidization so that the instant contact will be increased, but the contact number is decreased. These two factors together determine the means in Figure 13.

Clearly, coordination number, i.e., the number of contacts of a particle with its surrounding particles, is an important factor in describing the structure of a packed or fluidized bed. Thus, the final comparison in this work is focused on this parameter. For a system of two sized particles, there are three kinds of contacts, such as flotsam to flotsam, flotsam to jetsam or jetsam to flotsam, and jetsam to jetsam. This gives the so-called partial coordination numbers.[27,28] Figure 14 shows the variation of the mean partial coordination numbers with time at two velocity ratios. At a velocity ratio of 1.391, the mean partial coordination number between flotsam particles increases with time (line 1) and reaches its maximum when a macroscopically stable state is reached. The coordination between jetsam particles (line 2) also increases with time but reaches a constant value quickly, while the contact between jetsam and flotsam particles, which shows a higher number at the initial packing state, decreases with time. The mean value at the final macroscopically stable state from the 2D simulation is clearly lower than that from the 3D simulation. Almost no transition process can be found at velocity ratio 2.435, where the 3D simulation gives a higher value than the 2D simulation.

Time-averaged mean partial coordination numbers can provide a better comparison between the 2D and 3D simulations and are illustrated in Figure 15. For the mean contact number between flotsam particles (Figure 15a), both the 2D and 3D simulations show a decrease of the mean partial coordination number with the increase of gas velocity. Evidently, the 3D simulation shows a higher value than the 2D one at a given velocity ratio. This is also the case for the contact between jetsam particles (Figure 15b), but its value first increases, due to segregation with the increase of gas velocity, and then decreases due to strong fluidization with the further increase of gas velocity. For the contact between jetsam and flotsam particles (Figure 15c), the mean partial coordination numbers at a given velocity ratio are quite similar, but their trend is opposite to that in Figure 15b.

4. Conclusions

The wall effect on the fluidization behavior of a binary mixture is studied on the basis of the CCDM. The following conclusions can be drawn from this study.

(1) 2D and 3D packed/fluidized beds have quite different porosities, which does not make their direct comparison straightforward. Their comparison can be made against the ratio of the gas injection velocity to the minimum fluidization velocity.

(2) The mean kinetic energy of either flotsam or flotsam particles continuously increases with the increase of velocity ratio. Flotsam has a higher value than jetsam. At a given velocity ratio, a 2D simulation shows a higher value than a 3D simulation. The segregation spans in a larger range of velocities in 2D simulation than in 3D simulation.

(3) The mean drag forces acting on the flotsam and jetsam particles, as the sum of fluid drag and pressure gradient forces, are different at low and high gas velocity ratios, but identical

at the middle velocity ratios used in this study. For the gas dynamics expressed as the bed pressure drop in this study, the 3D simulation always shows a lower pressure drop than the bed weight, whereas for the 2D simulation, a continuous increase of pressure drop is observed, and at the highest velocity ratio, the pressure drop is even higher than the bed weight. This is because of the effect of particle−wall friction and the particle interlocking induced by the front and rear walls.

(4) A 3D simulation shows a larger contact potential between particles than a 2D simulation. This is also the case for the interaction with side and bottom walls. Overall, the contact number between particles in a 2D simulation is lower than in a 3D simulation.

(5) 2D and 3D simulations can produce results that are qualitatively similar. However, due to the effect of wall, the 2D results cannot fully represent the reality that is often 3D. Therefore, 3D modeling is necessary to produce quantitative results that can be used in an engineering application.

Acknowledgment

The authors are grateful to the Australia Research Council for the financial support of this work.

Literature Cited

(1) Patankar, S. V., *Numerical heat transfer and fluid flow*; Hemisphere: Bristol, PA, 1980.

(2) Cundall, P. A.; Strack, O. D. L. A discrete numerical model for granular assemblies. *Geotechnique* **1979**, *29*, 47–65.

(3) Tsuji, Y.; Kawaguchi, T.; Tanaka, T. Discrete particle simulation of two-dimensional fluidised bed. *Powder Technol.* **1993**, *77*, 79–87.

(4) Xu, B. H.; Yu, A. B. Numerical simulation of the gas-solid flow in a fluidised bed by combining discrete particle method with computational fluid dynamics. *Chem. Eng. Sci.* **1997**, *52*, 2786–2809.

(5) Yu, A. B.; Xu, B. H. Particle scale modelling of particle-fluid flow in fluidization. *J. Chem. Technol. Biotechnol.* **2003**, *78*, 111–121.

(6) Hoomans, B. P. B.; Kuipers, J. A. M.; Briels, W. J.; Van Swaaij, W. P. M. Discrete particle simulation of bubble and slug formation in a two-dimensional gas-fluidised bed: A hard-sphere approach. *Chem. Eng. Sci.* **1996**, *51*, 99–118.

(7) Zhu, H. P.; Zhou, Z. Y.; Yang, R. Y.; Yu, A. B. Discrete particle simulation of particulate systems: Theoretical developments. *Chem. Eng. Sci.* **2007**, *62*, 3378–3396.

(8) Zhu, H. P.; Zhou, Z. Y.; Yang, R. Y.; Yu, A. B. Discrete particle simulation of particulate systems: A review of major applications and findings. *Chem. Eng. Sci.* **2008**, *63*, 5728–5770.

(9) Hooman, B. P. B.; Kuipers, J. A. M.; Van Swaaij, W. P. M. Granular dynamics simulation of segregation phenomena in bubbling gas-fluidised beds. *Powder Technol.* **2000**, *109*, 41–48.

(10) Ouyang, J.; Li, J. Discrete simulation of heterogeneous structure and dynamic behavior in gas-solid fluidization. *Chem. Eng. Sci.* **1999**, *54*, 5427–5440.

(11) van Wachem, B. G. M.; van der Schaaf, J.; Schouten, J. C.; Krishna, R.; van den Bleek, C. M. Experimental validation of Lagrangian-Eulerian simulation of fluidized beds. *Powder Technol.* **2001**, *116*, 155–165.

(12) Zhou, H.; Flamant, G.; Gauthier, D.; Lu, J. Lagrangian approach for simulating the gas-particle flow structure in a circulating fluidized bed riser. *Int. J. Multiphase Flow* **2002**, *28*, 1801–1821.

(13) Bin, Y.; Zhang, M. C.; Dou, B. L.; Song, Y. B.; Wu, J. Discrete particle simulation and visualized research of the gas−solid flow in an internally circulating fluidized bed. *Ind. Eng. Chem. Res.* **2003**, *42*, 214–221.

(14) Feng, Y. Q.; Xu, B. H.; Zhang, S. J.; Yu, A. B.; Zulli, P. Discrete particle simulation of gas fluidization of particle mixtures. *AIChE J.* **2004**, *50*, 1713–1728.

(15) Feng, Y. Q.; Yu, A. B. An assessment of model equations in the discrete particle simulation of gas solid flow. *Ind. Eng. Chem. Res.* **2004**, *43*, 8378–8390.

(16) Feng, Y. Q.; Yu, A. B. Microdynamic modelling and analysis of the fluidisation and segregation of binary mixtures of particles. *Chem. Eng. Sci.* **2007**, *62*, 256–268.

(17) Gidaspow, D. *Multiphase flow and fluidization*; Academic Press: San Diego, 1994.

(18) Kafui, K. D.; Thornton, C.; Adams, M. J. Discrete particle-continuum fluid modelling of gas-solid fluidised beds. *Chem. Eng. Sci.* **2002**, *57*, 2395–2410.

(19) Di Felice, R. The voidage function for fluid-particle interaction systems. *Int. J. Multiphase Flow* **1994**, *20*, 153–159.

(20) Beetstra, R.; van der Hoef, M. A.; Kuipers, J. A. M. Numerical study of segregation using a new drag force correlation for polydisperse systems derived from lattice-Boltzmann simulations. *Chem. Eng. Sci.* **2007**, *62*, 246–255.

(21) Leboreiro, J.; Joseph, G. G.; Hrenya, C. M.; Snider, D. M.; Banejee, S. S.; Galvin, J. E. The influence of binary drag laws on simulations of species segregation in gas-fluidized beds. *Powder Technol.* **2008**, *184*, 275–290.

(22) Yin, X. L.; Sundaresan, S. S. Fluid-particle drag in low-Reynolds-number polydisperse gas-solid suspensions. *AIChE J.* **2009**, *55*, 1352–1368.

(23) Bridgwater, J.; Sharp, N. W.; Stocker, D. C. Particle mixing by percolation. *Trans. Inst. Chem. Eng.* **1969**, *47*, 114–119.

(24) Rahman, M.; Zhu, H. P.; Yu, A. B.; Bridgwater, J. DEM simulation of particle percolation in a packed bed. *Particuology* **2008**, *6*, 475–482.

(25) Marzocchella, A.; Salatino, P. Transient fluidization and segregation of binary mixtures of particles. *AIChE J.* **2000**, *46*, 2175–2182.

(26) Di Renzo, A.; Di Maio, F. P.; Girimonte, R.; Formisani, B. DEM simulation of the mixing equilibrium in fluidized beds of two solids differing in density. *Powder Technol.* **2008**, *184*, 214–223.

(27) Dodds, J. A. The porosity and contact points in multicomponent random sphere packings calculated by a simple statistic model. *J. Colloid Interface Sci.* **1980**, *77*, 317–327.

(28) Zou, R. P.; Bian, X.; Pinson, D.; Yang, R. Y.; Yu, A. B.; Zulli, P. Coordination number of ternary mixtures of spheres. *Part. Part. Syst. Charact.* **2003**, *20*, 335–341.

Received for review September 20, 2009
Revised manuscript received January 16, 2010
Accepted February 4, 2010

IE901478A